Article

Design and Reliability Analysis of a Series/Parallel Hybrid System with a Rotary Engine for Safer Ultralight Aviation

Teresa Donateo *[ID] and Ludovica Spada Chiodo [ID]

Department of Engineering for Innovation, University of Salento, Via per Monteroni, 73100 Lecce, Italy
* Correspondence: teresa.donateo@unisalento.it

Featured Application: Usage of series/parallel power systems for ultralight aviation to increase safety.

Abstract: The conventional powertrain for ultralight aviation consists of a fixed pitch propeller connected to an internal combustion engine (ICE). Since ICEs have a limited thermal efficiency (<40%), new and more efficient powerplant configurations have recently been proposed in the scientific literature by adopting hybrid electric solutions. Hybridization has the additional benefit of increased safety thanks to redundancy. This is a very important issue in ultralight aviation, where a high percentage of accidents are caused by engine failure. In a previous investigation, the authors proposed the design of a series/parallel hybrid electric power system to increase safety and optimize fuel economy by controlling the engine working points during flight. A new powertrain, derived from an automotive Honda i-MMD system, is analyzed in this study and a reliability analysis is performed to underline the improved safety obtained with the proposed system.

Keywords: hybrid electric aircraft; power split device; ultralight aviation; Wankel engine

1. Introduction

In the field of ultralight aviation, safety is a crucial topic. De Voogt et al. [1] reported that a large percentage of accidents that occurred in ultralight vehicles in Portugal, the USA, and the UK from 2000 to 2010 were the consequence of engine failure, and most of them occurred during ascent. To improve the safety of ultralight aviation, a hybrid electric propulsion system was developed in collaboration with Promecc Aerospace in a previous investigation by the authors [2], according to the technical standards defined by the Italian regulations for sport or leisure vehicles [3,4]. In particular, a series/parallel hybrid electric solution was designed in order to improve the safety and ensure a continuous ascent in a purely electric mode after engine failure. A second but not insignificant goal was the selection of relatively cheap technologies deriving from the automotive market.

A hybrid electric power system (HEPS) combines the advantages of conventional and all-electric power systems because it uses two or more power sources to produce propulsive power. Hybridization reduces fuel consumption and pollutant and acoustic emissions and generates very high power at take-off and ascent with respect to conventional power systems characterized by a single engine mechanically connected to a propeller [5]. With respect to an all-electric configuration [6], HEPSs increase the range and the endurance that are limited by the still insufficient energy density of today's batteries. HEPSs also have the advantage of redundance. In the case of engine failure, the electric drive can sustain the flight for a short time because of the possibility to "boost" the electric machine and the battery to work at their peak power.

According to the connection of the thermal and electric machines, HEPSs are classified as in parallel, series, and series/parallel [5].

In series HEVs, the generation of propulsive power is performed by the electric machine (motor). The required electric power comes from either the battery or from

another electric machine (generator) run by an internal combustion engine (electrical summation of power). The double conversion of power from mechanic-to-electric (in the generator) and electric-to-mechanic (in the motor) power and the large size of the electric machine connected to the output shaft are the main drawbacks of this configuration. On the other hand, there are two degrees of freedom in series HEPSs: the split of electrical power between the battery and the generator and the engine rotational speed. Therefore, it is possible to make the engine work at high efficiency in a large variety of operating conditions. This compensates for the negative effect of multiple energy conversions when the power request quickly varies, as in the case of an automobile running in an urban context.

Parallel HEPSs are characterized by a mechanical sum of the power of the engine and the electric machine at the transmission level. The single degree of freedom in a parallel configuration is the torque split between the engine and the motor, while the rotational speed of both converters is constrained by the output shaft speed. Unlike the series configuration, the parallel configuration requires only two converters (the engine and the electric machines) and they can be of smaller size because of the mechanical summation of power. In aerospace applications, piston engines are the most common choice, but a Wankel engine has been proposed in [7]. According to the authors of [8], parallel configurations can improve ascent performance by up to 56% and decrease the fuel consumption by 6% [5] with an increase of only 5% in weight compared to a non-hybrid system. In the case of failure of the engine or the motor, this configuration allows for the de-coupling of the combustion drivetrain or the shutting down of the electric power supply [9]. Unfortunately, if the accident takes place during take-off or ascent, this configuration is unable to give the required power because the engine and the electric machine are usually downsized in parallel HEPSs [10,11].

A series/parallel HEPS contains two electric power sources (the battery and the engine/generator system) and two mechanical power generation devices (the engine and the electric motor). The three machines are connected by a power coupling device. In the series/parallel configuration it is possible to optimize both the speed and the torque of the engine like in a series system. Similar to the parallel configuration, a series/parallel HEPS is based on the usage of smaller machines than a series arrangement.

There are two main types of power coupling devices for series/parallel hybrid electric vehicles [12]: the wet clutch (used in the Honda i-MMD [13]) and the planetary gearbox or power-split system such as in the Toyota THS [14–16]. Other more complex configurations have been proposed in the scientific literature, but they are unsuitable for aerospace applications, where it is mandatory to reduce the mass, bulk, and complexity. Both the Honda Hybrid System (HHS) and the THS allow the optimization of the engine working point; however, in the planetary systems, the engine is rigidly connected to the propulsion system to the detriment of driving comfort in the case of changing the engine start-stop mode (typical of the automotive applications).

In a previous investigation [2] performed on the same vehicle, the advantages of using a series/hybrid electric configuration to increase the safety and reduce fuel economy were addressed. This study adapted the THS system to an ultralight aerial vehicle and compared it with a conventional thermal powertrain adopting either a piston or a rotary engine. As in the original Toyota system [17], the engine is coupled with the carrier, the electric machine EM1 with the sun gear, while the electric machine EM2 is on the outer gear (see Figure 1). The same electric machines of the original THS were considered, while the piston engine was replaced by a rotary thermal machine.

A Wankel engine [2] was preferred for this application because of its high power/weight ratio and simple design. Similar to all rotary engines, the thermodynamic cycle of a Wankel is not obtained from the reciprocating movement of a piston in a cylinder. The four stages of intake, compression, ignition, and exhaust, in fact, are achieved by the movement of an eccentric rotor within an epi-trochoidal housing. Wankel engines are characterized by a low maintenance cost thanks to the reduced number of moving parts and the absence of intake and exhaust valves, while the rotary kinematics decrease noise and vibrations. The

drawbacks of Wankel engines are related to the large surface-to-volume ratio and to the slow rotation of the rotor chamber (one-third of the eccentric shaft speed). These features intensify the wall heat flux and reduce the thermal efficiency of the engine. Moreover, Wankel engines suffer from sealing problems and low power outputs at low speeds [18]. These problems can be partially solved by the use of a hybrid electric power system, especially in a series configuration [19].
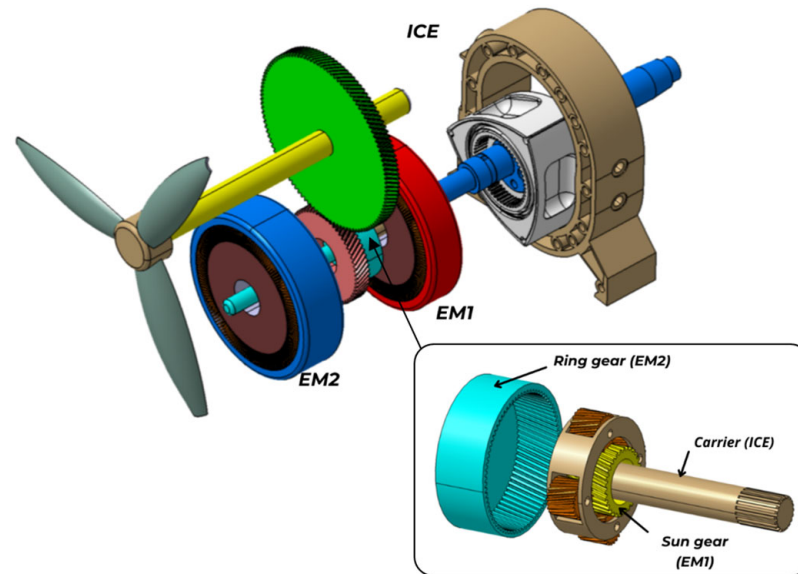

Figure 1. Toyota powersplit adopted in a previous investigation [2].

The results of the previous study releveled that, even accounting for a larger take-off mass and despite the lower efficiency of the Wankel engine, the proposed HEPS allowed an improvement in the fuel consumption of about 20%. Compared with a non-hybrid Wankel engine arrangement, the series/parallel HEPS improved the fuel economy by 28%. These fuel saving figures were estimated with a backward simulation approach starting from a typical mission and calculating the consumption of fuel and electricity (in the hybrid case). Stationary performance curves and efficiency maps were used for the propeller, the engine, and the electric machines.

A planetary gear configuration allows high torque transmission and a large speed reduction to be achieved with relatively small gears, as required by the automotive application. However, its complex design and manufacturing tend to make it a more expensive solution than other gearbox types and its configuration makes heat dissipation more difficult. Other disadvantages are the high bearing load, inaccessibility, and design complexity [20]. Moreover, it requires a complex energy management strategy. For these reasons and for the fact that it is impossible to disengage the engine in case of failure, the Honda system was adopted in this investigation and a preliminary Honda-type series/parallel hybrid configuration was designed. To the authors' knowledge, this system has never been considered for aerospace applications.

Another contribution of this investigation is represented by the reliability analysis. As stated in [21], the reliability of HEVs has not been investigated deeply until now, due to the fact that hybrid technology is at an early stage of development, together with the amount of time required to collect data related to component and subsystem reliability, which in addition are often retained as proprietary information. However, the authors of [21] claim the superiority of ICE-based vehicles in terms of reliability, only considering the lower number of system components. The possibility of working under partial functionality of hybrid systems must be considered, which is a crucial aspect in making them more reliable than conventional systems.

A reliability assessment has been carried out, considering the importance of attaining a higher safety level as a key objective of the present study. The reliability assessment proposed in this investigation is based on the well-known Markov models [22], but the present investigation introduces a complete calculation of series/parallel system reliability, which includes not only propulsion system components but also the clutch and the gearbox to give an indication of the behavior of the entire system that will be developed.

The novelty and potential impact of the proposed investigation on the scientific literature on this topic is also guaranteed by the adoption of a series/parallel configuration (that is quite overlooked in the hybridization of aircraft) and by the sizing procedure which is based on the analysis of the power request under a realistic mission according to different energy management strategies.

The rest of the paper is organized as follows: Section 2 defines the reference ultralight airplane and the modeling approach; Section 3 describes the sizing of the series/parallel power system and its operating modes. Finally, Section 4 reports the results of the reliability analysis, the details of which are described in Appendix A.

2. Ultralight Aircraft and the Modeling Approach

In this investigation, the retrofitting of the Promecc Aerospace Freccia to a hybrid electric ultralight aircraft was performed. The aircraft has a take-off mass of 450 kg and a wing area of 12 m^2 (see Figure 2). The HEPS was designed and simulated according to the realistic flight mission shown in Figure 3 that was obtained from a previous investigation [23].

Figure 2. Reference aircraft (Promecc Aerospace Freccia).
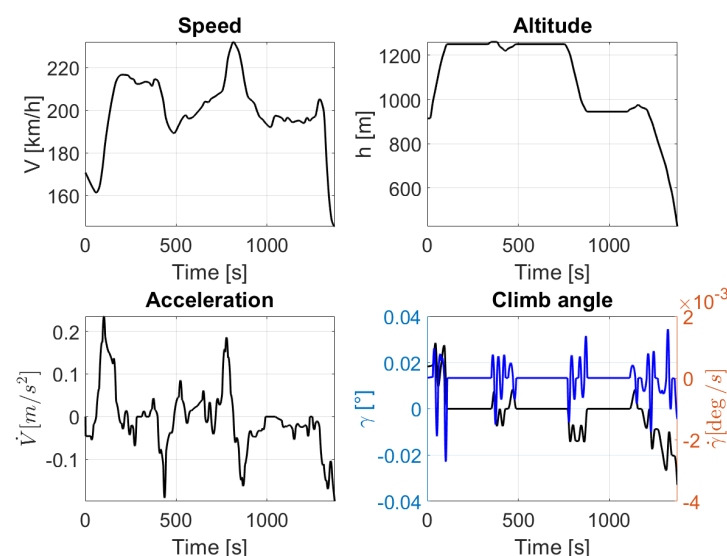

Figure 3. Mission profile.

The original configuration for the Freccia includes a fixed pitch propeller. This kind of propeller works at high efficiency in a very limited operating range. High pitch propellers

are preferred because they improve efficiency during cruising [24], which is the longest phase of flight and the most significant for fuel consumption. However, the reduced efficiency during ascent leads to a higher power demand that results in the need to increase the installed power and this, in turn, causes a higher takeoff weight [25]. Moreover, the engine efficiency is constrained in a conventional power system by the need to follow the speed and torque demands of the propeller. Therefore, the engine is sized according to the takeoff and ascent power and then works at partial load during the cruise and in the final part of the flight (descent).

A variable pitch propeller maintains the ideal blade setting for each flight phase by adjusting the pitch position [25] by means of a push–pull rod driven by a servo [26] or a governor. In this way, the propeller rotation speed can be kept constant (constant speed propeller) [27]. Even if constant speed operation does not warrant optimal propeller efficiency, it allows the engine to be operated at constant speed and expands the propeller's operating range, allowing it to absorb the maximum engine power [28].

In this investigation, a fixed speed propeller with a diameter of 1.78 m with the dimensionless performance map of Figure 4 was considered. By applying the balance of forces acting on the plane along the mission and by using the following polar, $C_D = 0.0349 + 0.0749C_L^2$, as suggested in [29] for an ultralight aircraft, the propulsive power request was calculated. By dividing the propulsive power by the efficiency of the propeller, it was possible to obtain the power request at the output shaft of the series/parallel power system, which is reported in Figure 4, together with the propulsive power. More details on the evaluation of the propulsive power can be found in [23].
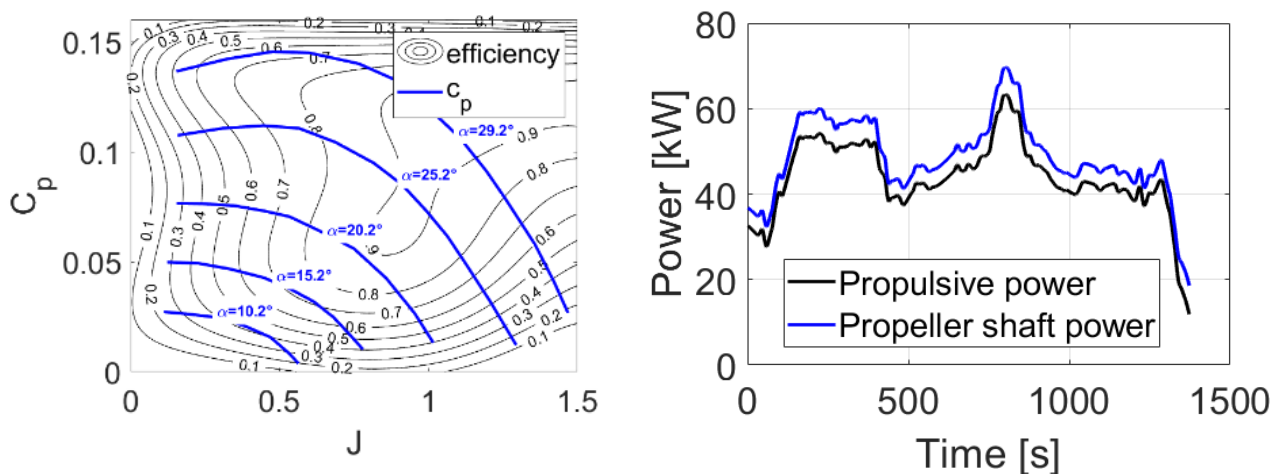

Figure 4. Propeller efficiency map (**left**) and propulsive vs. shaft power (**right**).

The shaft power request in Figure 4 must be satisfied each time by the hybrid electric power system according to the selected operating mode (as explained in the next section). The thermal and electric machines are modeled by means of performance curves and efficiency maps available in the scientific literature. In particular, the wide-open throttle torque curve and the efficiency map of the Wankel engine, reported in Figure 5, are obtained from the two-rotor Mazda 13B [30]. The optimal operating line (OOL) shown in the figure collects all the torque and speed combinations that, for a specific power request, guarantee the minimum fuel consumption in steady-state conditions.

Generic Brushless DC electric machines were considered in this investigation. Their efficiency map is obtained with a simple Willans line approach as suggested in [31]. More details on the simulation approach can be found in [2]. Note that this kind of approach is universally accepted in the preliminary design of hybrid electric power systems when experimental data are not available [31].
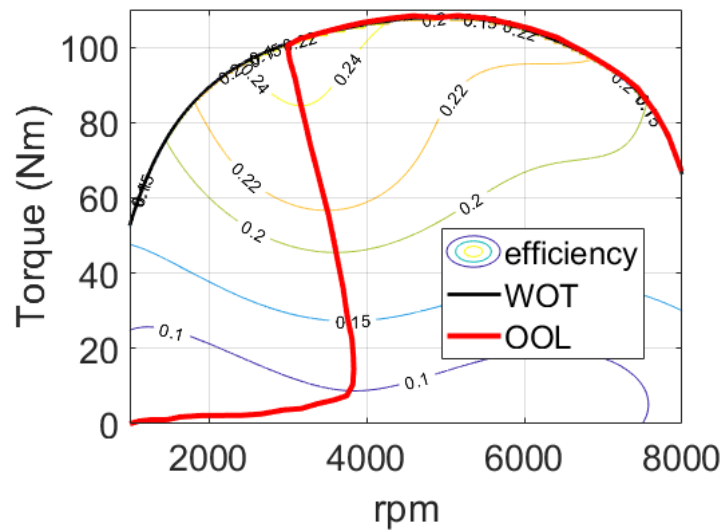
Figure 5. WOT torque curve (black line), efficiency map (isoline map), and OOL(red line) of the Wankel engine at sea level.

3. The New Power System

In this investigation, the Wankel engine is connected with a new power split device to the two electric machines that, unlike the previous power system [2], are not obtained from the Toyota Prius configuration, but sized according to the mission requirements and operating mode as explained later in the paper.

3.1. Transmission Scheme and Operating Modes

Many of the power split devices proposed for the automotive field are very complex, characterized by the presence of many planetary gears and clutches (see, for example, patents US 11,305,636 and 2008/0248909). On the contrary, the Honda i-MMD presents a lower degree of complexity while maintaining high flexibility in the choice of the engine working point, and is therefore considered suitable for the present application. The Honda i-MMD system was proposed in 2013 and makes use of four pairs of gears and one clutch that allows the decoupling of the internal combustion engine from the transmission [32]. This system will be henceforth named HHS (Honda hybrid system).

The operating modes of the HHS are schematized in Figure 6. When the clutch is open, the system works in electric vehicle mode or in series HEV, while the second electric machine propels the vehicle. When the clutch is locked, the vehicle operates in parallel mode and the engine speed is proportionate to the wheel speed.
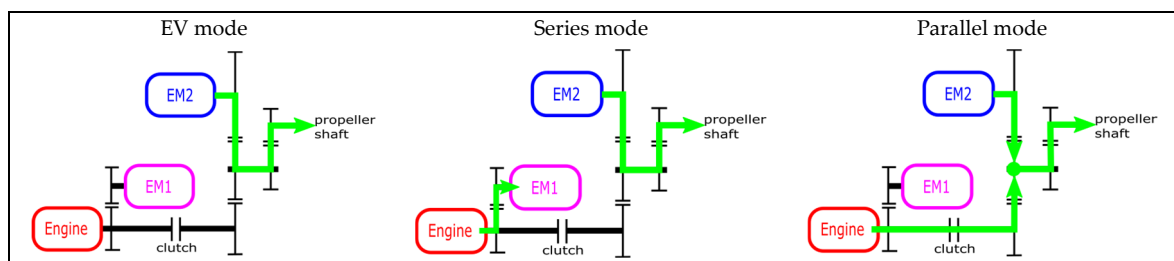

Figure 6. Working modes of the Honda hybrid system.

As shown in Figure 7, the shafts of the electric motor EM2 and generator EM1 are coaxial. A clutch is interposed between gear 6 and gear 7 to allow the internal combustion engine to be decoupled, while the latter is always in mesh with the generator shaft via gear 6.
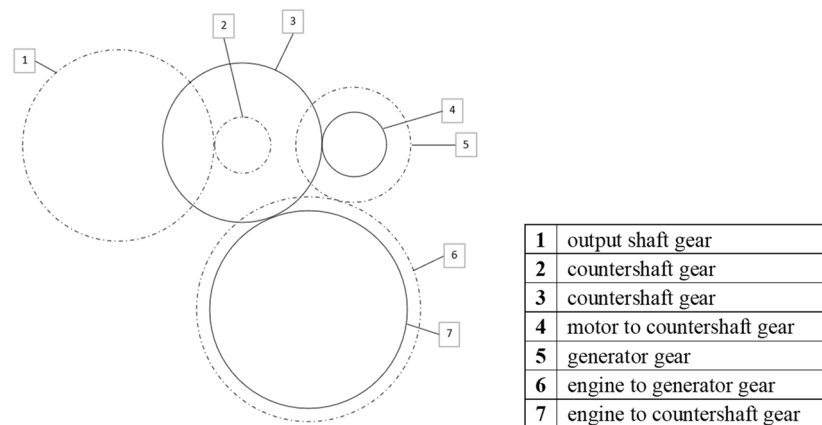
1	output shaft gear
2	countershaft gear
3	countershaft gear
4	motor to countershaft gear
5	generator gear
6	engine to generator gear
7	engine to countershaft gear

Figure 7. Transmission scheme of the HHS.

3.2. Choice of the Rotational Speeds

To adapt the system to the present application, the wheel shaft was replaced by a propeller shaft and the transmission was subjected to a first preliminary design, which led to the modification of the transmission ratios to make them more suitable for use with a variable pitch propeller, and thus at a given output shaft speed. Given the configuration chosen for the transmission, the speeds and torque ranges were obtained for the engine and electric motors, respectively, in engine mode and EV series mode when the engine is decoupled from the transmission shaft.

The second step in the design process was to evaluate the choice of the engine speed on the basis of its performance curve and efficiency map at sea level (Figure 5).

The wide-open throttle (WOT) power of the engine is 70 kW and is reached at the speed of 7000 rpm, while the WOT torque is maximized at 4700 rpm. Therefore, if the transmission is designed so that the engine runs at 7000 rpm, the mission can be entirely performed in thermal mode and the engine power is fully exploited. Actually, it would be necessary to take into account the reduction in WOT power that is caused by the lower pressure and temperature of the atmosphere at the flight altitude. For naturally aspirated engines, such a reduction can be expressed as [33]:

$$\frac{BHP(z)}{BHP(0)} = 1.13\sigma(z) - 0.13 \tag{1}$$

where *z* is the flight altitude, *BHP* is the engine WOT brake horsepower, and "σ(z)" is the ratio between air density at *z* and air density at sea level (z = 0).

Figure 8 shows the percentage of loss of engine WOT power as a function of the flight altitude. Keeping in mind the mission in Figure 3, a 10% loss in the engine is obtained for the specific application.

However, in order to reduce fuel consumption, it could be suitable to make the engine work at its best efficiency point (optimal operating point, OOP), but in this case, the sea level power should be only 30 kW. To compromise between performance and efficiency, a rotational speed of 4590 rpm was chosen for the Wankel engine. The relevant operating points of the engine considered in this investigation are summarized in Table 1.

Table 1. Relevant engine working points.

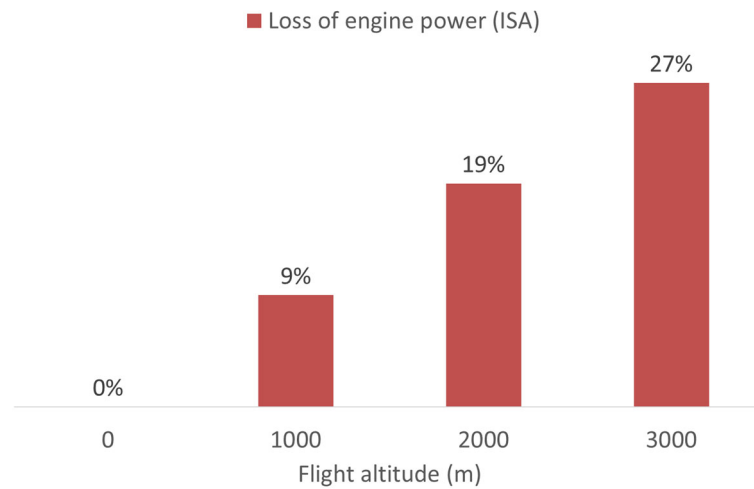| Operating Point	Speed (rpm)	Torque (Nm)	Power (kW)	Efficiency (%)
Max power (WOT)	7000	95.5	70.0	0.220
Max torque (WOT)	4700	109.0	53.7	0.230
Best efficiency (OOP)	3000	95.0	29.8	0.240
WOT and OOL @ selected speed	4590	107.7	51.8	0.235

Figure 8. Loss of engine power as a function of flight altitude.

As for the electric machines, the speeds of EM1 and EM2 were chosen with a trial-and-error procedure considering a constant output speed of 2000 rpm. The geometrical and functional limits of the proposed power split device and the range of feasibility of permanent magnet machines were taken into account in the procedure. The results of the analysis led to the choice of 8570 rpm for EM2 and 7000 rpm for EM1. The number of teeth and the transmission ratio of the original and modified systems are reported in Table 2.

Table 2. Number of teeth (z) and transmission ratios (τ).

	z1	**z2**	**z3**	**z4**	**z5**	**z6**	**z7**	**τ21**	**τ43**	**τ73**	**τ65**
Original Honda iMMD	65	19	54	22	39	76	69	3.42	2.43	0.81	0.51
Adapted HHS	50	28	36	15	21	32	28	1.79	2.4	1.29	0.66

3.3. Energy Management and Power Sizing

In the previous investigation, a complex energy management strategy was proposed to allow the engine to work at optimal operating points independently of the propeller speed and torque request. In the new configuration, thanks to the constant speed of the propeller, the energy management can be simplified.

The size of the electric machines and the battery were obtained from the power request distribution among the engine and the electric machines according to the three operating modes of the system.

- Full electric: the engine is disengaged and no fuel is used;
- Hybrid power assist: the mission is performed with the engine running at 4590 rpm. The EM2 machine is used help the engine when the shaft power overcomes $51.8 \cdot [1.13\sigma(z) - 0.13]$ kW, i.e., the maximum power that the engine is able to deliver at that speed at altitude z (see Table 1 and Equation (1));
- Hybrid series: the engine is disengaged from the transmission so that its operating point can be set equal to the OOP of Table 1. The engine power is delivered to the generator (EM1), which in turn supplies electric power to the motor (EM2). If insufficient, additional power is delivered to EM2 from the battery. On the contrary, when the EM1 power is higher than the shaft power request, the excess power is store in the battery.

The power distribution among the different machines and the battery according to these operating modes is reported in Figure 9. The mission cannot be performed in thermal mode (using only the engine) with the selected engine speed. However, to obtain a term for a comparison of fuel saving, the engine is assumed to be running at its max power

rotational speed (7000 rpm), thus obtaining a hypothetical thermal mode where only the engine is used to move the propeller.
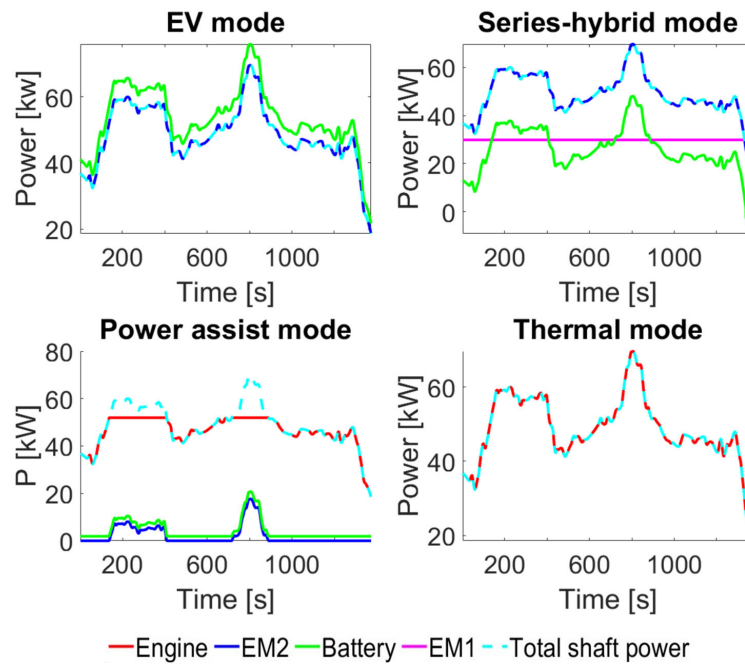

Figure 9. Distribution of power among the different components of the power system.

The plots in Figure 9 were obtained by taking into account the efficiency of the three machines. For the engine, the efficiency was obtained from the map of Figure 5, while the electric machines were modelled with a Willans line model. For details of the modelling approach, please refer to [2].

The results of the mission analysis are reported in Table 3. The table reports the consumption of fuel and electricity of the HHS with the three possible operation modes, the consumption of a hypothetical thermal configuration with the engine allowed to run at 7300 rpm (max power), and the consumptions obtained with the THS over the same mission with the same take-off mass.

Table 3. Consumption of fuel and electricity for different operating modes.

Operating Mode	Fuel Consumption	Electricity Consumption
HHS—EV	-	20.5 kWh
HHS—POWER ASSIST MODE	8.5 L	1.6 kWh
HHS—SERIES HYBRID MODE	5.8 L	9.8 kWh
THERMAL (hypotethical)	10.7 L	-
THS (old powertrain)	5.6 L	3.9 kWh

Compared with the thermal hypothetical mode, the HHS in power assist mode allows a fuel saving of about 20%, while needing a very small battery to account for the electricity consumption. On the other hand, a fuel saving of about 45% can be obtained with the series hybrid mode, but this would require a much larger battery (about 10 kWh). With twice this size of the battery, the mission could be performed in all-electric mode.

The improvement in fuel economy guaranteed by the series hybrid mode is due not only to the reduced contribution of the engine in satisfying the shaft power request, but also to the higher and constant efficiency of the engine that works always at its OOP while in power assist mode, the engine works at 4590 rpm (see Table 1). The time trends of engine efficiency in the series hybrid, power assist, and thermal cases are compared in Figure 10.
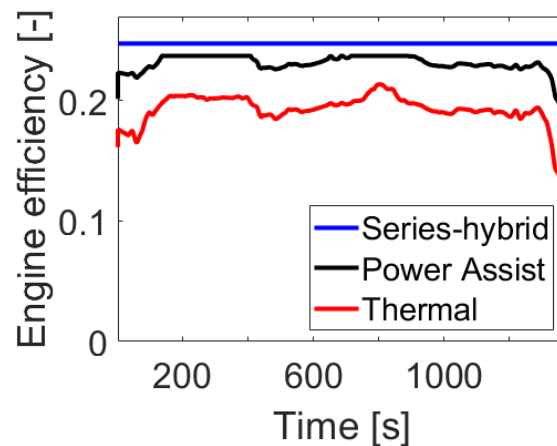
Figure 10. Engine efficiency for the series -hybrid, power assist, and thermal modes.

With respect to the previous powertrain (THS + constant pitch propeller) with the complex energy management strategy explained in [2], the HHS causes an increase in both fuel consumption and electricity consumption. However, as already pointed out, the new system is less complex and the engine works at constant torque and speed.

To complete the sizing of the electric machines, the mission requirements were taken into account and translated to the minimum size of the electric machines. The minimum size of machine EM2 is 69.6 kW in EV, while 17.7 kW is sufficient in power assist mode. The machine EM1, that works only in series hybrid mode, has a minimum size of 30 kW.

Table 4 compares the new power system, sized according to the series hybrid mode, with that proposed in the previous study. The only difference is the larger size of electric machine EM2. However, EM2 works at constant speed in the new systems thanks to the adoption of a constant speed propeller, while its rotational speed was variable in the THS system because of the fixed pitch propeller.

Table 4. Specifications of the old and new powertrains.

	Specification	Toyota Hybrid System (THS)	Honda Hybrid System (HHS)
Wankel engine	Peak power	70 kW @ 7000 rpm	70 kW @ 7000 rpm
	Displacement	654 cm^3	654 cm^3
	Fuel	Avgas	Avgas
EM1	Max. power	30 kW	30 kW
EM2	Max. power	50 kW	70 kW

3.4. Battery Sizing and Weight Considerations

The battery must be sized by considering not only the limitations in terms of gravimetric energy density but also in terms of power density [34]. Assuming a depth of discharge of 80% and a gravimetric energy density of 200 Wh/kg for the battery, the battery mass ranges between 10 kg for the power assist mode and 128 kg for the all-electric case. As a compromise, the battery size will be set equal to 10 kWh (62.5 kg) because, in case of engine failure, the aircraft can easily complete takeoff and ascent and then descend to land. Since the maximum battery power in Figure 9 is about 76 kW, the battery must have a power density of about 1200 W/kg, a value in line with today's high-power lithium battery technology [33].

At this stage, an accurate weight analysis of the proposed system has not yet been performed, even if for each component, the weight can be estimated from the literature data of power densities for modern electric machines. However, it is not correct to evaluate the weight of a hybridization scheme by simply adding the weight of the extra components to the original weight of the aircraft [35]. First, the starter motor/generator and the battery of

the conventional configuration are not needed anymore to turn on the engine and generate on-board electricity. In the case under analysis, moreover, the proposed power system makes use of a very light Wankel engine, and the fuel saving can help reduce the size of the fuel tanks. Additionally, note that, according to Italian legislation, the takeoff weight must be kept under 450 kg, which is also the actual takeoff weight of the reference vehicle used in this investigation. Therefore, the retrofitting of the Freccia would not be feasible even with a limited increase in the powertrain weight. For this reason, the design of a new prototype ultralight aircraft will be the goal of the next step of this project, which will also include a reduction in the weight and bulk of the proposed system and the choice of battery.

4. Reliability Analysis

Once the proposed propulsive system was outlined, a reliability analysis was carried out, as flight safety enhancement was the main objective of the present research. To this end, a Markov model has been used, as suggested in [22].

According to this approach, the reliability of a system is calculated in terms of availability as the probability of existing in a state of usability, which is based on the transition rates from a pre-existent "healthy state" and the transition rates from a previously failed to a "healthy" state in each time interval.

In its simplest form, the availability of the system in Figure 11 is given by the probability associated with the state "healthy", while the transition from one state to the other is characterized by the parameters λ and μ, which are failure and repair rates, respectively, defined as:

$$\lambda = \frac{1}{\text{MTBF}} \tag{2}$$

$$\mu = \frac{1}{\text{MTTR}} \tag{3}$$

where MTBF and MTTR are the mean time between failure of and the mean time to repair a given component.
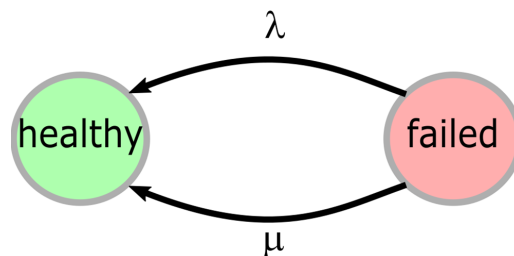

Figure 11. Markov chain of a two-state system.

In complex systems such as that being examined, a reliability assessment is related to the particular configuration of the system itself, so that all possible states can be enumerated and consequently their probability can be calculated. In the present work, the reliability of the developed system is compared to the reference conventional system, which is the system before hybridization.

The conventional system (only thermal) is made of three distinct components, namely the engine, the clutch, and the gearbox. It follows that the system can assume eight different states, summarized in Table 5, where the working state of a component or system is denoted by 1 and the failed state by 0 and whose transitions are represented in Figure 12.

Thus, the availability of the system coincides with the probability of state 1, calculated as:

$$P_1 = \frac{\mu_E \cdot \mu_C \cdot \mu_{GB}}{(\mu_E + \lambda_E) \cdot (\mu_C + \lambda_C) \cdot (\mu_{GB} + \lambda_{GB})} \tag{4}$$

where the subscripts E, C, and GB of failure rate, λ, and repair rate, μ, refer to the engine, clutch, and gearbox, respectively. From Equation (4), an availability of 0.9910 is obtained.

Table 5. States of the conventional system.

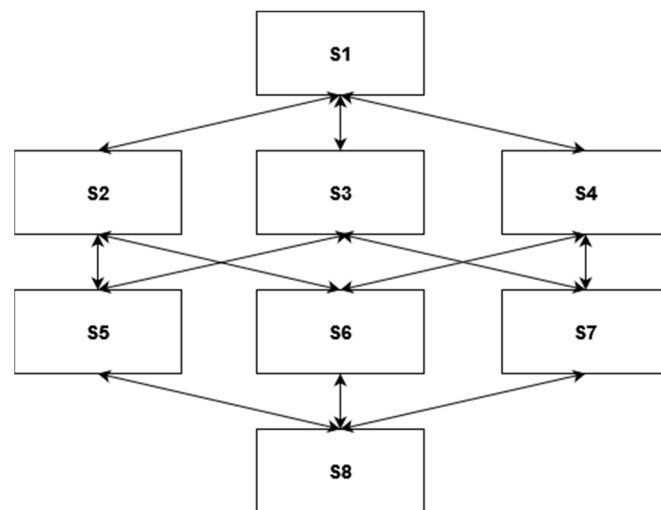| State Number	Condition	Engine	Clutch	Gearbox	System
1	Healthy system	1	1	1	1
2		1	1	0	0
3	Single fault	1	0	1	0
4		0	1	1	0
5		1	0	0	0
6	Dual fault	0	1	0	0
7		0	0	1	0
8	Three faults	0	0	0	0

Figure 12. Markov chain of the conventional system.

As the hybrid system is made of six components (battery, EM2, EM1, engine, clutch, and gearbox), the number of states is now 64. The states and the corresponding Markov chain for the proposed hybrid system are given in Appendix A. It is assumed that gearbox failure always leads to system failure, while clutch failure is not critical, as long as the system can work in electric mode. The failure and repair rates employed in the calculation of system availability are given in Table 6 [22,36,37].

Table 6. Failure and repair rates of involved components.

	λ (1/y)	μ (1/y)
Engine	2.52802	361.6846
Generator (EM1)	0.01111	4151.659
Battery	0.0006	848.0155
Motor (EM2)	0.01825	2591.716
Clutch	0.032259	16.10294
Gearbox	0.2545	3981.818

The availability of the hybrid system, calculated as the sum of the probabilities of the working system states, is equal to 0.9999.

As expected, the redundancy and versatility of the hybrid system allow for a higher availability with respect to the conventional system, demonstrating the efficacy of hybridization in increasing safety.

Additionally, the reliability of the system in conventional, series, and parallel configurations has been calculated over a time horizon of t = 1000 h, according to the following equations:

$$R = e^{\lambda t} \ \text{(component reliability)} \tag{5}$$

$$R_{series} = R_1 \cdot \ldots \cdot R_n \ \text{(reliability of a system made of n components in series)} \tag{6}$$

$$R_{parallel} = 1 - \prod_{i=1}^{n}(1 - R_i) \ \text{(reliability of a system made of n components in parallel)} \tag{7}$$

The results are given in Table 7, which reaffirms the advantage of hybridization. Both the power assist and series configurations increase the reliability by 33% with respect to the conventional power system.

Table 7. Reliability of different system configurations.

Configuration	Reliability
Conventional	0.72519
Series hybrid	0.969327
Power assist	0.970835

Note that the reliability analysis performed in this investigation does not take into account the replacement of the piston engine with a rotary one, because the data on the reliability of a Wankel engine in the scientific literature are limited and controversial. On the one hand, the Wankel engine has a very limited number of moving parts with respect to a piston configuration, and the study of Yewale et al. [38] demonstrated that this kind of engine is able to complete endurance testing. On the other hand, this kind of engine experiences trouble with the sealing of the trochoidal rotor and stress in the eccentric shaft [39].

5. Conclusions

The preliminary design and the reliability analysis of a hybrid electric power system for the retrofitting of an ultralight airplane were addressed in this paper. The goals of the preliminary design were three: ensuring the safety of aircraft operation in case of engine failure, proposing a less complex power split device with respect to a previous investigation of some of the authors, and saving fuel despite the usage of a low-efficiency type of engine (Wankel). The results of the present investigation showed that all these goals can be achieved with series/parallel power systems, a configuration hitherto neglected in the aerospace industry. In particular, it was found that a series/parallel configuration with an adapted Honda hybrid system increases the reliability by 33% with respect to the conventional configuration. The simplicity of the device was guaranteed by replacing the planetary system with a helical gearbox used in a previous study and by considering a fixed speed propeller that also allows obtaining a relevant fuel saving (with respect to a full thermal configuration) with a very simple energy management strategy. The battery and the electric machines were sized by considering the power request of the power system in three different operating modes: all-electric (in case of engine failure), power assist (parallel), and series. In further investigations, a new aircraft prototype will be designed and the proposed power system will be optimized with the goal of reducing the weight and bulk in order to meet the requirements of maximum take-off weight for ultralight aviation according to Italian legislation.

Author Contributions: Conceptualization, T.D. and L.S.C.; methodology, T.D.; software L.S.C.; investigation, T.D. and L.S.C.; writing—original draft preparation, T.D. and L.S.C.; writing—review and editing, T.D.; supervision T.D.; project administration, T.D. All authors have read and agreed to the published version of the manuscript.

Institutional Review Board Statement: Not applicable.

Informed Consent Statement: Not applicable.

Data Availability Statement: The data presented in this study are available on request from the corresponding author. The industrial partner's policy prevents public access to the data.

Conflicts of Interest: The authors declare no conflict of interest.

Appendix A

Table A1. States of the proposed series parallel hybrid system (E = engine; EM1 = generator; B = battery; EM2 = motor; C = clutch; GB = gearbox; S = system).

State Number	Condition	E	EM1	B	EM2	C	GB	S
1	Healthy	1	1	1	1	1	1	1
2		0	1	1	1	1	1	1
3		1	0	1	1	1	1	1
4	Single fault	1	1	0	1	1	1	1
5		1	1	1	0	1	1	1
6		1	1	1	1	0	1	1
7		1	1	1	1	1	0	0
8		0	0	1	1	1	1	1
9		0	1	0	1	1	1	0
10		0	1	1	0	1	1	0
11		0	1	1	1	0	1	1
12		0	1	1	1	1	0	0
13		1	0	0	1	1	1	1
14		1	0	1	0	1	1	1
15	Dual fault	1	0	1	1	0	1	1
16		1	0	1	1	1	0	0
17		1	1	0	0	1	1	1
18		1	1	0	1	0	1	1
19		1	1	0	1	1	0	0
20		1	1	1	0	0	1	0
21		1	1	1	0	1	0	0
22		1	1	1	1	0	0	0
23		0	0	0	1	1	1	0
24		0	0	1	0	1	1	0
25		0	0	1	1	0	1	1
26		0	0	1	1	1	0	0
27		0	1	0	0	1	1	0
28		0	1	0	1	0	1	0
29		0	1	0	1	1	0	0
30		0	1	1	0	0	1	0
31	Three faults	0	1	1	0	1	0	0
32		0	1	1	1	0	0	0
33		1	0	0	0	1	1	1
34		1	0	0	1	0	1	0
35		1	0	0	1	1	0	0
36		1	0	1	0	0	1	0
37		1	0	1	1	0	0	0
38		1	1	0	0	0	1	0
39		1	1	0	0	1	0	0

Table A1. *Cont.*

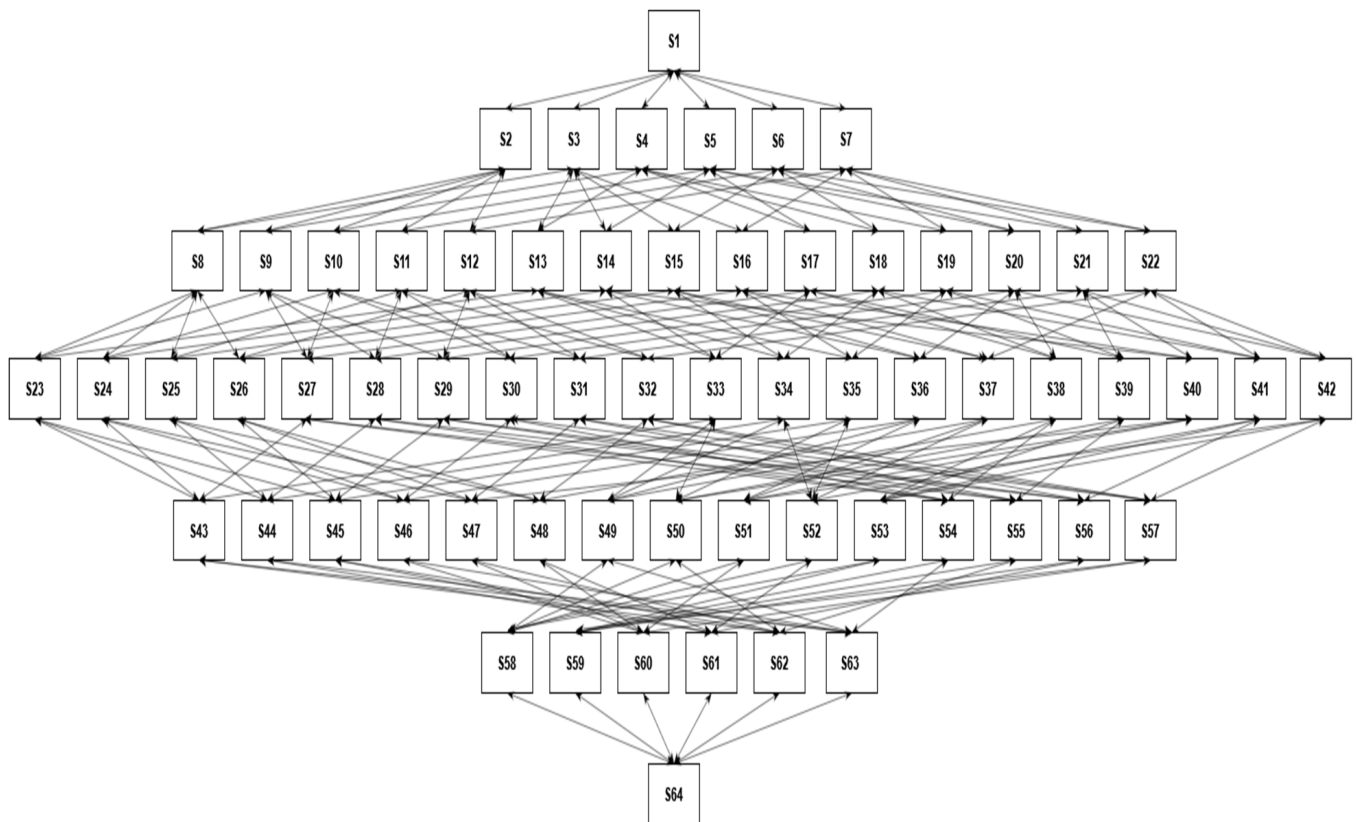| State Number	Condition	E	EM1	B	EM2	C	GB	S
40		1	0	1	0	1	0	0
41		1	1	0	1	0	0	0
42		1	1	1	0	0	0	0
43		0	0	0	0	1	1	0
44		0	0	0	1	0	1	0
45		0	0	0	1	1	0	0
46		0	0	1	0	0	1	0
47		0	0	1	0	1	0	0
48		0	0	1	1	0	0	0
49		1	0	0	0	0	1	0
50	Four faults	1	0	0	0	1	0	0
51		1	0	1	0	0	0	0
52		1	0	0	1	0	0	0
53		1	1	0	0	0	0	0
54		0	1	0	0	0	1	0
55		0	1	0	0	1	0	0
56		0	1	0	1	0	0	0
57		0	1	1	0	0	0	0
58		1	0	0	0	0	0	0
59		0	1	0	0	0	0	0
60		0	0	1	0	0	0	0
61	Five faults	0	0	0	1	0	0	0
62		0	0	0	0	1	0	0
63		0	0	0	0	0	1	0
64	Six faults	0	0	0	0	0	0	0

Figure A1. Markov chain of the proposed series parallel HEPS.

References

1. De Voogt, A.; Chaves, F.; Harden, E.; Silvestre, M.; Gamboa, P. Ultralight Accidents in the US, UK, and Portugal. *Safety* **2018**, *4*, 23. [CrossRef]
2. Donateo, T.; Cavalera, D. Increasing Safety in Ultralight Aviation with a Wankel-Based Series/Parallel Hybrid Electric Power System. *Machines* **2022**, *10*, 486. [CrossRef]
3. Decreto del Presidente della Repubblica. 9 luglio 2010, n. 133. Available online: https://www.gazzettaufficiale.it/eli/id/2010/0 8/19/010G0149/sg (accessed on 31 October 2021).
4. Decreto Ministeriale. n. 503 del 10/12/2021. Available online: https://www.mit.gov.it/normativa/decreto-ministeriale-numero-503-del-10122021 (accessed on 31 March 2022).
5. Hung, J.Y.; Gonzalez, L.F. On parallel hybrid-electric propulsion system for unmanned aerial vehicles. *Prog. Aerosp. Sci.* **2021**, *51*, 17. [CrossRef]
6. Alshahrani, A. Analysis and Initial Optimization of the Propeller Design for Small, Hybrid-Electric Propeller Aircraft. Master's Thesis, KTH Royal Institute of Technology, Stockholm, Sweden, 2020.
7. Bongermino, E.; Mastrorocco, F.; Tomaselli, M.; Monopoli, V.G.; Naso, D. Model and Energy Management System for a Parallel Hybrid Electric Unmanned Aerial Vehicle. In Proceedings of the 2017 IEEE 26th International Symposium on Industrial Electronics (ISIE), Edinburgh, UK, 19–21 June 2017; pp. 1868–1873. [CrossRef]
8. Glassock, R.; Hung, J.Y.; Gonzalez, L.F.; Walker, R.A. Design, modelling and measurement of a hybrid powerplant for unmanned aerial systems. *Aust. J. Mech. Eng.* **2008**, *6*, 69–78. [CrossRef]
9. Friedrich, C.; Robertson, P.A. Hybrid-electric propulsion for automotive and aviation applications. *CEAS Aeronaut. J.* **2015**, *6*, 279–290. [CrossRef]
10. Hasseliquist, A.; Baker, S.P. Homebuilt Aircraft Crashes. *Aviat. Space Environ. Med.* **1999**, *70*, 543–547.
11. Pagán, B.J.; De Voogt, A.J.; Van Doorn, R.R. Ultralight aviation accident factors and latent failures: A 66-case study. *Aviat. Space Environ. Med.* **2006**, *77*, 950–952. [PubMed]
12. Yang, Q.; Dai, X.; Wu, G. Clutch Coordination Control for Series-Parallel DHT Mode Changing. *SAE Tech. Pap.* **2022**, *1*, 7046. [CrossRef]
13. Higuchi, N.; Sunaga, Y.; Tanaka, M.; Shimada, H. Development of a new two-motor plug-in hybrid system. *SAE Int. J. Altern. Powertrains* **2013**, *2*, 135–145. [CrossRef]
14. Rousseau, A.; Kwon, J.; Sharer, P.; Pagerit, S.; Duoba, M. Integrating Data, Performing Quality Assurance, and Validating the Vehicle Model for the 2004 Prius Using PSAT, SAE Technical Paper 2006-01-0667. In Proceedings of the SAE 2006 World Congress & Exhibition, Detroit, MI, USA, 3–6 April 2006.
15. Burress, T.A.; Campbell, S.L.; Coomer, C.L.; Ayers, C.W.; Wereszczak, A.A.; Cunningham, J.P.; Marlino, L.D.; Seiber, L.E.; Lin, H.T. *Evaluation of the 2010 Toyota Prius Hybrid Synergy Driver System, ORNL/TM-2010/253*; Oak Ridge National Laboratory: Oak Ridge, TN, USA, 2011.
16. 2004 Toyota Prius-1052 Hybrid Battery Test Results. Available online: https://avt.inl.gov/sites/default/files/pdf/hev/batteryprius1052.pdf (accessed on 3 April 2022).
17. Xu, X.; Zhao, J.; Shi, K.; Dong, P.; Wang, S.; Liu, Y.; Guo, W.; Liu, X. Comparative study on fuel saving potential of series-parallel hybrid transmission and series hybrid transmission. *Energy Convers. Manag.* **2022**, *252*, 114970. [CrossRef]
18. Amrouche, F.; Erickson, P.; Park, J.; Varnhagen, S. An experimental investigation of hydrogen-enriched gasoline in a Wankel rotary engine. *Int. J. Hydrog. Energy* **2014**, *39*, 8525–8534. [CrossRef]
19. Varnhagen, S.; Same, A.; Remillard, J.; Park, J.W. A numerical investigation on the efficiency of range extending systems using Advanced Vehicle Simulator. *J. Power Sources* **2011**, *196*, 3360–3370. [CrossRef]
20. Shah, N.; Prajapati, R.; Dabhi, H.; Patel, J. Design of A Hybrid Transmission for Electric and Engine Powered Transmission. *Int. J. Eng. Res. Technol. (IJERT)* **2019**, *8*, 378–388.
21. Mi, C.; Masrur, M.A. *Hybrid Electric Vehicles: Principles and Applications with Practical Perspectives*, 2nd ed.; Wiley: Hoboken, NJ, USA, 2018.
22. Negarestani, S.; Ghahnavieh, A.R.; Mobarakeh, A.S. A Study of the Reliability of Various Types of the Electric Vehicles. In Proceedings of the IEEE International Electric Vehicle Conference, Greenville, SC, USA, 4–8 March 2012; pp. 1–6. [CrossRef]
23. Donateo, T.; Totaro, R. Hybridization of training aircraft with real world flight profiles. *Aircr. Eng. Aerosp. Technol.* **2019**, *91*, 353–365. [CrossRef]
24. Riboldi, C.E.D. An optimal approach to the preliminary design of small hybrid-electric aircraft. *Aerosp. Sci. Technol.* **2018**, *81*, 14–31. [CrossRef]
25. Ma, S.; Wang, S.; Zhang, C.; Zhang, S. A method to improve the efficiency of an electric aircraft propulsion system. *Energy* **2017**, *140*, 436–443. [CrossRef]
26. Stevenson, R.; Chandra, C.; Christon, J.; Wiryanto, W.; Virginio, R.; Adiprawita, W. Energy consumption comparison of static pitch propeller and variable pitch propeller using maximum thrust equation approach in small scale electric unmanned aerial vehicle. *AIP Conf. Proc.* **2020**, *2226*, 020001. [CrossRef]
27. Filippone, A.; Barakos, G. Rotorcraft systems for urban air mobility: A reality check. *Aeronaut. J.* **2021**, *125*, 3–21. [CrossRef]
28. McDonald, R.A. Optimal Propeller Pitch Scheduling and Propeller—Airframe Matching for Conceptual Design. In Proceedings of the AIAA congress 2015-3190, Session: Transformational Flight—Electric Propulsion, Dallas, TX, USA, 22–26 June 2015. [CrossRef]

29. Martínez Ruiz, L. Estudio de Viabilidad: Oxicombustión con Producción de Oxígeno Embarcada en Aviación General. Grado en Ingeniería Aeroespacial. Universitat Politècnica de València. 2021. Available online: http://hdl.handle.net/10251/171250 (accessed on 3 April 2022).
30. Ansdale, R.F.; Lockley, D.J. *The Wankel RC Engine, Design and Performance*; ILIFE Books: London, UK, 1968.
31. Guzzella, L.; Sciarretta, A. *Vehicle Propulsion Systems: Introduction to Modeling and Optimization*; Springer: Berlin, Germany, 2013.
32. Jeong, J.; Karbowski, D.; Rousseau, A.; Rask, E. Model Validation of the Honda Accord Plug-In. *SAE Tech. Pap.* **2016**, *1*, 1151. [CrossRef]
33. Taylor, C.F. *The Internal-Combustion Engine in Theory and Practice*; MIT Press: Cambridge, MA, USA, 1985; Volume 1.
34. Wang, X.-T.; Yang, Y.; Guo, J.-Z.; Gu, Z.-Y.; Ang, E.H.; Sun, Z.-H.; Li, W.-H.; Liang, H.-J.; Wu, X.-L. An advanced cathode composite for co-utilization of cations and anions in lithium batteries. *J. Mater. Sci. Technol.* **2022**, *102*, 72–79. [CrossRef]
35. Olsen, J.; Page, J.R. Hybrid powertrain for light aircraft. *Int. J. Sustain. Aviat.* **2014**, *1*, 85–102. [CrossRef]
36. Hendry, M.B.; Zekas, M.B. U.S. Navy Experience with SSS (Synchro-Self-Shifting) Clutches. *Mech. Eng.* **2010**, *132*, 54–55. [CrossRef]
37. Repin, S.; Evtiukov, S.; Maksimov, S. A method for quantitative assessment of vehicle reliability impact on road safety. *Transp. Res. Procedia* **2018**, *36*, 661–668. [CrossRef]
38. Yewale, G.; Tapkire, A.; Radhakrishna, D.; Shejwal, P.; Singh, K.; Panchal, G. Endurance Testing for Wankel Rotary Engine. *SAE Tech. Pap.* **2017**, *26*, 0336. [CrossRef]
39. Cihan, O.; Bulut, M.; Kutlar, O.A. Stress analysis of a Wankel engine eccentric shafts under varied thermal conditions. *Mater. Test.* **2019**, *61*, 1157–1164. [CrossRef]